Sustainable Marine Structures
https://ojs.nassg.org/index.php/sms

ARTICLE

Thermocline Model for Estimating Argo Sea Surface Temperature

Chunling Zhang[1*] Mengli Zhang[1] Zhenfeng Wang[2] Song Hu[1] Danyang Wang[1] Shenglong Yang[3*]

1. College of Marine Science, Shanghai Ocean University, Shanghai, 201306, China
2. Project Management Office of China National Scientific Seafloor Observatory, Tongji University, Shanghai, 200092, China
3. Key Laboratory of East China Sea & Oceanic Fishery Resources Exploitation and Utilization, Ministry of Agriculture, Shanghai, 200090, China

ARTICLE INFO

Article history
Received: 28 December 2021
Accepted: 4 January 2022
Published Online: 14 January 2022

Keywords:
Argo
Sea surface temperature
Thermocline model
The Pacific Ocean

ABSTRACT

Argo has become an important constituent of the global ocean observation system. However, due to the lack of sea surface measurements from most Argo profiles, the application of Argo data is still limited. In this study, a thermocline model was constructed based on three key thermocline parameters, i.e, thermocline upper depth, the thermocline bottom depth, and thermocline temperature gradient. Following the model, we estimated the sea surface temperature of Argo profiles by providing the relationship between sea surface and subsurface temperature. We tested the effectiveness of our proposed model using statistical analysis and by comparing the sea surface temperature with the results obtained from traditional methods and in situ observations in the Pacific Ocean. The root mean square errors of results obtained from thermocline model were found to be significantly reduced compared to the extrapolation results and satellite retrieved temperature results. The correlation coefficient between the estimation result and in situ observation was 0.967. Argo surface temperature, estimated by the thermocline model, has been theoretically proved to be reliable. Thus, our model generates theoretically feasible data present the mesoscale phenomenon in more detail. Overall, this study compensates for the lack surface observation of Argo, and provides a new tool to establish complete Argo data sets.

*Corresponding Author:
Chunling Zhang,
College of Marine Science, Shanghai Ocean University, Shanghai, 201306, China;
Email: clzhang@shou.edu.cn
Shenglong Yang,
Key Laboratory of East China Sea & Oceanic Fishery Resources Exploitation and Utilization, Ministry of Agriculture, Shanghai, 200090, China;
Email: ysl6782195@126.com

DOI: http://dx.doi.org/10.36956/sms.v4i1.474

1. Introduction

Global Argo array, consisting of more than 3000 profiling floats, has become an important constituent of the global ocean observation system. They are configured and pumped to ensure the highest quality data acquisition from global ocean. To avoid the degradation of salinity accuracy owing to sea surface contaminants, the pump is turned off at ~5 dbar beneath the sea surface as the Argo float ascends. Therefore, the conventional Argo floats obtain temperature and salinity measurements from depths of ~5- 2000 m. Although sea surface temperature (SST) is the key indicator of climate change, it is integral for both ocean circulation and climate change studies [1]. The combination of Argo and satellite SST has been used in several studies [2-4], even though neither the spatial nor the temporal resolution of the two data sets are similar.

A SST salinity (STS) sensor, developed by Sea-Bird Electronics Inc., was used on the Argo float and in the Aquarius Sea Surface Salinity Mission, to measure SST and salinity. This sensor can be used in conjunction with the main SBE-41 CP CTD installed in an Argo float [5]. The STS sensor samples at 1 Hz concurrently with the SBE-41 CP CTD near the float park depth (960- 980 dbar) and subsequently in the upper ocean (3- 20 dbar) just before the SBE-41 CP is turned off. With the increasing demands of such new Argo floats, a large number of near-surface temperature and salinity data are expected to be generated for ocean and atmospheric research. However, the stability of the new Argo floats with STS sensor still needs to be significantly improved. The STS sensor were first put into use in October, 2008; however, by the end of 2020, the number of STS sensors launched by international Argo plan member countries was still <1000. At present, near-surface temperature and salinity data are significantly lesser compared to that required for climate prediction and data assimilation. Therefore, it is necessary to use statistical methods to estimate SST with the help of Argo subsurface data.

It is necessary to assimilate Argo alone or in combination with other observations to generate gridded dataset with the aid of data assimilation techniques, which can be directly used for studies [6]. Due to the lack of surface measurements, some Argo gridded dataset considers 5 m (the nearest surface observation depth of traditional Argo float) as the first surface layer without using additional data [7,8]. Most of Argo datasets consider satellite SST or the added surface measurement data obtained from observation stations as the surface data [9-12]. Roemmich and Gilson obtained Argo observations at ~0–2000 m by linear interpolation and generated climate data for 58 vertical depths [13]. Some other scholars used satellite SST directly, for determining surface temperature of Argo dataset or adopted Akima's extrapolation method to obtain SST [14,15].

The increasing volume of in situ observations are far behind that of Argo. Moreover, in situ data cannot match the increasing volume and temporal length of Argo observations in the near future. In the past few decades, the satellite derived SST has become a primary data source owing to its global spatial coverage and high temporal resolution, however, it is not based on in situ measurements. The retrieved satellite data is significantly different from SST measured in situ at depths of ~0.2- 2 m [16]. The simple combination of satellite SST and Argo subsurface data produces large errors [17]. Several studies employ widely used extrapolation techniques, which are simple method and provide a rough estimation of temperature and salinity. To avoid these short-comings, we propose a parametric model based on thermocline parameters. The SST in the Pacific Ocean was estimated using the subsurface Argo data to verify the accuracy of this model. The Argo observations and the principle of the used method are described in Section 2. In Section 3, we verify our results, and apply them to discuss the thermocline and vertical temperature structure in section 4. Finally, in section 5, we present our conclusions.

2. Materials and Methods

2.1 Data Processing

Three types of marine data are open-accessed for worldwide research, including Argo subsurface profiles, Global Temperature and Salinity Profile Project (GTSPP) data, and Argo Near-surface Temperature (Argo NST). The traditional Argo profiles used to calculate the model parameters were provided by China Argo Real-time Data Center (ftp://ftp.argo.org.cn/pub/ARGO/global/). Due to the dependence of our proposed methods on thermocline parameters, test data that reflect notable thermocline characters are required. Considering the number of Argo observations, data from August, 2020 was chosen as the test data. The test data consisted of a total of 12,726 profiles measured during August, 2020 in the Pacific Ocean (Figure 1a). The data passed a series of quality control tests, such as the test of observation parameters and layers, land, ocean and region detection, density inversion test, the test of range of temperature and salinity, and time judgment [18]. Meanwhile, the estimated SST from Argo subsurface data depended on the initial depth as different reference layers provided different results. These results were weighted by comparing with GTSPP sea surface observations obtained from buoy stations at

depths of ~0.2- 2 m. The GTSPP profiles are obtained from National Oceanic and Atmospheric Administration (NOAA) (http://data.nodc.noaa.gov/gtspp/best.nc/). After removing duplicate data, a total of 6230 profiles during August, 2020, which were mostly located in the equatorial Pacific region was obtained (Figure 1b).

Argo NST observation was used to verify the results estimated from our proposed model. Argo NST data of the same period are available on the National Oceanography Centre's (NOC) ftp website (ftp://ftp.pol.ac.uk/pub/bodc/argo/NST/). These floats with non-pumped near-surface temperatures are deployed and processed by the British Oceanographic Data Centre, the Indian National Centre for Ocean Information Services, the Japan Meteorological Agency, the Scripps Institution of Oceanography, and the University of Washington, respectively. Collectively, a total number of 540 profiles were used in this study, and most of them were primarily located in the western part of the Pacific Ocean (Figure 1b).

2.2 Thermocline Model

The model proposed in this study estimates the SST base at the mixed layer depth (MLD) or the thermocline upper depth, the thermocline bottom depth (TBD), and thermocline temperature gradient (TTG). These key parameters were calculated by the maximum angle method [19-21]. The proposed model was improved and a new application in estimating Argo surface temperature. We constructed the model depicted in Equation (1) by considering the minimal possible degrees of freedom. Figure 2 illustrates the principle behind the proposed model. The estimated SST of Argo from subsurface temperature was different for different reference layers. In this study, 10 m, 20 m, 30 m, 50 m, 75 m, 100 m, 125 m, 150 m, and 200 m were chosen as reference layers to estimate SST in the Pacific Ocean. Subsequently, nine different temperatures measured at each grid were averaged according to (Equation 2):

$$\begin{aligned} SST &= \frac{P_0}{P_z} T_z, \qquad (0 \le z \le \mathrm{MLD}) \\ SST &= T_z - \mathrm{TTG}(z - \mathrm{MLD}), \quad (\mathrm{MLD} \le z \le \mathrm{TBD}) \end{aligned} \tag{1}$$

$$SST_i = \frac{\sum_{j=1}^{9} b_{i,j} SST_{i,j}}{\sum_{j=1}^{9} b_{i,j}}, \qquad b_{i,j} = \exp(-(r_{i,j} - \bar{r}_i)^2 / L^2) \tag{2}$$

where SST is sea surface temperature. Tz is the subsurface temperature at the depth of z estimated by Argo temperature profile data. The parameters P0 and Pz represent sea surface and subsurface pressure, respectively. To ensure the continuity of Tz and Tz' (the differential of Tz) at TBD, the temperature function at depth below the TBD was adopted as gauss function $T_z - T_d = (T_{td} - T_d)\exp[\frac{z_0^w - (z_0 + z + \mathrm{TBD})^w}{H^w}], (z \ge \mathrm{TBD})$, similar to that used in previous work [19]. H^W is the depth scale and Ttd is the temperature at TBD obtained by dichotomy. Td is the temperature in the deepest layer. Base on continuity T(TBD+0)=T(TBD-0) and $\frac{dT(\mathrm{TBD}+0)}{dz} = \frac{dT(\mathrm{TBD}-0)}{dz} = \mathrm{TTG}$, differentiation of the gauss function with respect to z is $z_0 = [\frac{HG_{th}}{w(T_{th} - T_d)}]^{1/(w-1)}$.

The w parameter should be less than 1, otherwise, z_0 becomes significantly large, and temperature starts decreasing with depth. Table 1 shows the root mean square errors (RMSEs) of the estimated results with different W and *H*. When W is constant, the RMSE values decrease initially, and subsequently increases. The RMSE values are least value when *H*=2000 m. Moreover, *H* is constant

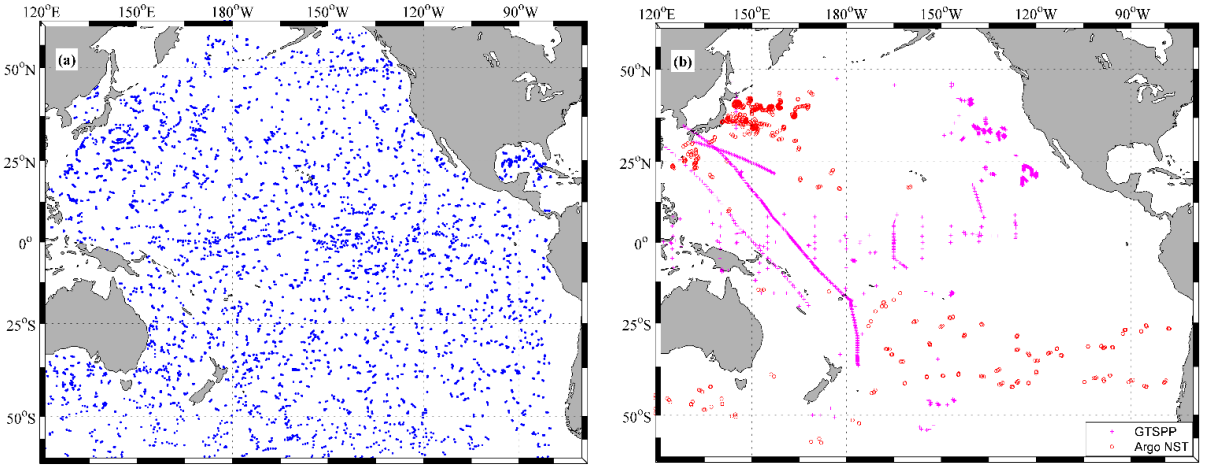

Figure 1. Locations of Argo subsurface profiles (a), and (b) GTSSPP or Argo near surface observations.

and the RMSEs of the estimated temperatures are the least when W=0.5. Hence, W and *H* were set as 0.5 and 2000 m, respectively, to ensure the least RMSE at a temperature of 0.637 °C. SSTi is the estimated SST at the i th section of the Argo profile. SSTi,j is the estimated temperature at ith profile according to jth (j=1,2,…9) datum layer. rij is the RMSE for SSTi, j and GTSPP data. The different results at different starting depth have minimum temperature RMSE compared with GTSPP when the correlation scale *L* has a value of 2 degrees (Figure 3).

2.3 Algorithm of Thermocline Parameters

To estimate the SST by Equations (1) and (2) described in section 2.2, the key parameters—MLD, TBD, TTG should be determined. The maximum angle method [20,21], a simple and objective method, was adopted to calculate these parameters with the Argo dataset of August, 2020. It not only uses the main feature (vertically uniform) of the mixed layer (i.e., temperature (or density) deviation and vertical gradient criteria) but also uses the main characteristics of the thermocline (sharp gradient) beneath the mixed layer. However, this method can be improved, when the variable is strictly monotonous, the depth of density mixed layer is regarded as isothermal layer depth.

To ensure a monotonous profile, the maximum angle method of the potential density profile was used to determine thermocline parameters via Argo observations. Figure 4 illustrates the methodology used by a potential density profile. The vertical density difference represents the total variability of potential density. Theoretically, the variability of the vertical density difference is approximately zero in the constant-density layer, and it becomes larger in the pycnocline beneath the mixed layer. It is reasonable to identify the main parts of the pycnocline between the two depths. The main depths were set corresponding to 10% and 70% difference in vertical density. The MLD and TBD were determined between the main depths by point to point linear polynomial fitting. Figure 4 provides a schematic representation of the vector fitting used in our proposed method. At depth z_k (marked by a circle in Figure 4), both vectors (downward positive) were constructed by linear polynomial fitting of the profile data from z_{k-1} to z_k. The subscript k increases downward with k = 1 at the surface or at the nearest location to the surface. In the constant-density (isothermal) layer, the angle θ reaches its maximum value (see Figure 4b), and is smaller if z_k is inside (Figure 4a) or outside (Figure 4c) the

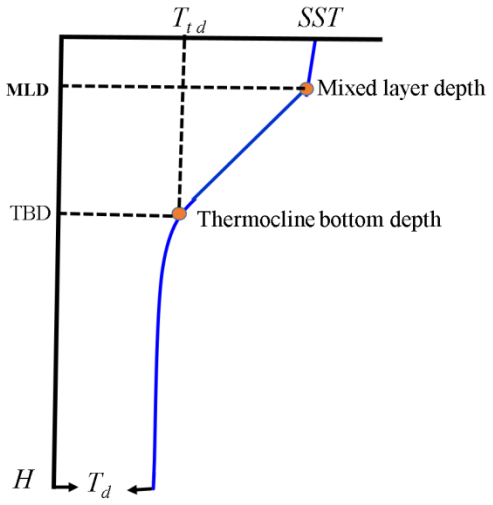

Figure 2. Principle of thermocline parametric model. SST denotes sea surface temperature. The parameters h1, h2 and H represent mixed layer depth, thermocline bottom depth, and depth scale, respectively.

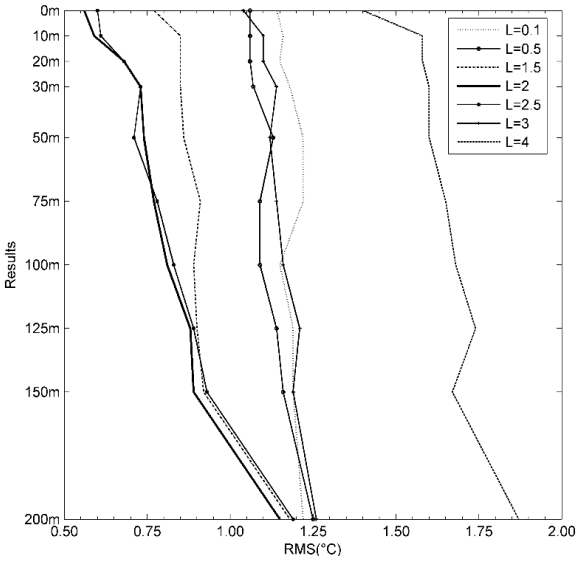

Figure 3. Different RMSEs of SST (°C) for different correlation scale L.

Table 1. Estimated RMSEs of SST (°C) with different *W* and *H* values

	$W = 0.1$	$W = 0.25$	$W = 0.5$	$W = 0.6$	$W = 0.8$
***H*=1000 m**	1.123	0.971	0.805	0.812	0.877
***H*=1500 m**	0.908	0. 884	0.795	0.819	0.830
***H*=2000 m**	0.782	0.761	**0.637**	0.800	0.802
***H*=3000 m**	0.851	0.780	0.711	0.873	0.935
***H*=5500 m**	0.893	0.852	0.790	0. 963	1.020

mixed layer. Thus, the maximum angle principle can be used to determine the mixed layer depth (θmax, $MLDz_k$). In practice, the angle θ is difficult to calculate, therefore, tan θ was used instead.

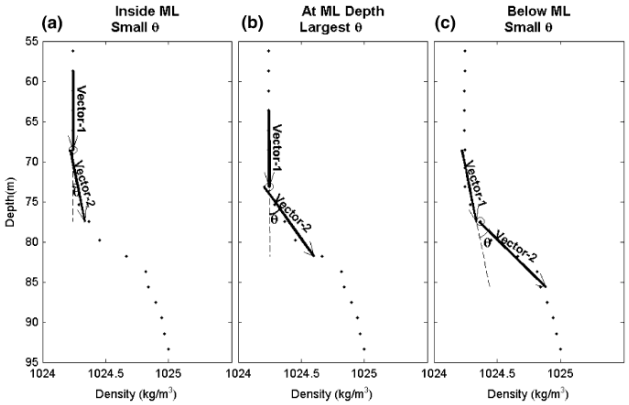

Figure 4. Illustration of the max angle method. The dots represent density of each depth. The vector angles (indicated by θ) have small value inside or outside the mixed layer depth ((a) and (c)), and it has the largest value at the depth of thermocline upper depth.

In order to ensure the stability of the simulation results from the sbPOM model, the time of the outer mode (positive compression mold) was set to 20 s and the time of the inner mode (oblique compression mold) was set to 600 s. The bathymetric topography was based on the General Bathymetry Chart of the Oceans (GEBCO), which has a minimum water depth of 10 m. The maximum water depth was set to 5000 m, and water depths exceeding 5000 m were replaced by 5000 m to match the maximum water depth in the SODA data. The spatial resolution of the simulated sea surface temperature from the sbPOM model is a 0.25° grid at a 1-hour interval.

3. Validation of the Results

3.1 Correlation Analysis

The estimation of SST from subsurface temperature using the thermal parametric model (Figure 2) is based on the hypothesis proposed by Chu and Fan [20]. The linear correlation coefficient between SST anomaly and MLD anomaly is significantly larger than that between SST anomaly and other parameters, i.e., $|r_1|>|r_2|$, $|r_1|>|r_3|$in formula $MLD'=r_1SST'$, $TBD'=r_2SST'$, $TTG'=r_3SST'$ where, r_1, r_2, r_3 are the regression coefficients of MLD', TBD', TTG', respectively. The parameter anomalies (SST', MLD', TBD', TTG') were obtained from the thermal parameters (SST, MLD, TBD, TTG) by subtracting their mean values within a 1o×1o grid cell at each observation locations.

Figure 5 shows the scatter plot between SST' and (MLD', TBD', TTG') in the Pacific Ocean. The data points concentrate around the fitting line in Figure 5a. Although the data points in Figure 5b and 5c plot relatively far away from the fitting line, three absolute values of r obtained by linear regression indicate that MLD' has the largest correlation coefficient with SST' among all subsurface parameters. The correlation coefficients between SST' and MLD', TBD', and TTG' were 0.249, −0.046, and 8.334e-04, respectively. The significance of the correlation was evaluated by statistical analyses $t=\frac{r\sqrt{n-2}}{\sqrt{1-r^2}}$, where the t distribution had a degree of freedom of n-2. Here, r is the correlation coefficient and n is the number of analyzed samples (19,200). The critical value of t at significance level of 0.005 was 2.576 ($t_{0.005}$ (19200-2)=2.576). Three absolute values of t between SST' and MLD', TBD', and TTG' were 1.832, –0.326, and 0.059, respectively. These values were less than the critical value of 2.576. In other words, we can suggest that the analyzed data are within the uncertainty of the statistical test.

From the above analysis, we conclude that the correlation coefficient between the two short timescale parameters SST' and MLD' is significantly larger than that between SST' and the long timescale parameters (TBD', TTG'). This in turn theoretically confirmed the reliability of estimating SST based on thermal parametric model in the Pacific Ocean.

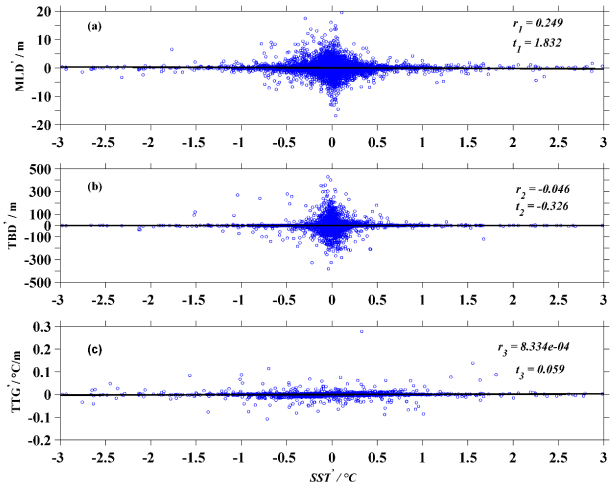

Figure 5. Correlation analysis between sea surface temperature anomaly and thermocline parameter anomaly. (a) The correlation coefficients between sea surface temperature anomaly and mixed layer depth anomaly, (b) thermocline bottom depth anomaly, and (c) thermocline gradient are represented by r1, r2, and r3, respectively. The parameter t indicates t-critical at significance level of 0.005.

3.2 Comparison with Observations

The commonly used methods to obtain Argo surface temperature include extrapolation method proposed by Akima [22] and satellite derived SST. According to the thermocline model (described in 2.2), the estimation of SST was based on reference layers (10 m, 20 m, 30 m, 50 m, 75 m, 100 m, 125 m, 150 m, 200 m) and different results were weighted by gauss function. Next, we compared the temperature results from the different datum layers, the thermocline model (recorded as SST), Akima extrapolation (named as extra), and satellite AMSR-E SST (indicated by satellite) by considering the data obtained from GTSPP and Argo NST observations as true values.

Table 2 lists the RMSEs of temperature estimated from the nine different datums, weight-averaged SST based on Equation (2), the surface temperature obtained by extrapolation (extra) and satellite AMSR-E SST (satellite) compared with GTSPP and Argo NST. It is evinced that the temperature RMSEs increase with the datum depth in the results obtained from thermocline model. The weighed-averaged SST has smaller RMSE of 1.04 °C and 0.99 °C compared to that of GTSPP and Argo NST, respectively. However, the RMSEs of estimated temperatures corresponding to the nine datum layers were all less than 1.6 °C for the two base datasets. The RMSEs between the extra surface temperature and the two practical datasets have a value of >1.8 °C, which are larger than all estimations. The RMSEs between the satellite AMSR-E SST and the two practical datasets are ~2 °C and 1.5 °C relative to GTSPP and Argo NST, respectively. Although both GTSPP and Argo NST are sparse and asymmetrical in space, Table 2 illustrates that the SST estimated by thermocline parametric model is more close to in situ observation compared to satellite and extra. Meanwhile it indicates that weighted mean method (formula (2)) can improve the accuracy of estimation. Moreover, the in situ Argo NST and GTSPP data were not used during the estimation process, as discussed below. Thus, the test was strictly independent.

The correlation analysis results and absolute temperature errors of SST derived from thermocline model SST (Figure 6a), extrapolated results (indicated by extra in Figure 5b), and satellite derived (Figure 6 c) are displayed in Figure 6. Figures 6(a1), (b1), and (c1) provide the correlation coefficient R, RMSE, regression line, and its confidence interval with confidence level of 90%. It is evident that SST in the Pacific Ocean is in better agreement with Argo NST compared to extra or satellite. The SST data points concentrate around the fitting line $y = 0.99x + 1.05$, and have the smallest residual standard deviation (S = 1.72) compared to other methods. The correlation coefficient between SST and Argo NST was 0.967, which is smaller than the other results. The distribution of extra and satellite data points are more dispersed, with linear fitting coefficients of 0.87 and 0.89, respectively. Both extra and satellite derived results have high correlation with the Argo NST with correlation coefficients of 0.911 and 0.937, respectively. However, their RMSEs were significantly larger than that of SST. The maximum absolute temperature errors of thermocline model shown in Figure 5 a2 are <1 °C. In fact, most of the errors in the estimated temperature were <0.5 °C. There are a few profiles near 40 °N with temperature errors of ~ 1 °C. Most of the errors in temperature estimated by extrapolation and satellite based were >1.5 °C, with the maximum error exceeding 2.5 °C in the Northwest Pacific.

Argo NST data shown in Figure 6 are sparse in the equatorial region. The GTSPP observations were primarily obtained from the anchor buoys in tropical Pacific. Figure 7 shows the absolute temperature errors between the different results and GTSPP in the equatorial Pacific. The temperature errors of SST obtained from the thermocline model (Figure 7a) were minor at all observation locations. Most of the SST errors were <0.5 °C with a few temperature errors being in the range of 0.5- 1.0 °C. In contrast, the errors in temperature of extra and satellite displayed a skewed distribution, especially in the extrapolation results (Figure 7b). Most of these errors in extra temperature exceed 1.5 °C and half of the total errors were approximately at 2.5 °C. In the satellite results (Figure 7 b), the errors in temperature were concentrated at 0.5–2.0 °C, which are smaller than that obtained in the extra results but larger than in the thermocline model SST errors. Thus, both theoretical statistics and observation comparisons show that the thermocline model can provide more accurate results.

4. Discussion

4.1 Thermocline Parameters Analysis

Three thermocline parameters involved in this study

Table 2. RMSEs of the estimated temperature (°C) for different SST and in situ observation

Results	10m	20m	30m	50m	75m	100m	125m	150m	200m	SST	Extra	Satellite
GTSPP	1.13	1.15	1.18	1.10	1.20	1.52	1.59	1.44	1.51	1.04	1.94	1.96
Argo NST	1.04	1.21	1.21	1.16	1.26	1.28	1.35	1.48	1.54	0.99	1.84	1.50

vary with respect to different timescales. The MLD has a short correlation timescale. On the other hand, the TBD and TTG have longer correlation timescales. The strongest thermocline in the northern hemisphere and the weakest in the southern hemisphere appears during August [23]. This is reflected from the distribution of thermocline parameters of August, 2020 obtained from Argo profiles and gridded by the optimal interpolation [24,25] (Figure 8).

There are more than 60% MLDs lesser than 100 m as obtained by Argo profiles. Most of them are in the Northern Pacific (Figure 8 (a1)). The MLD in the Southern Pacific are concentrated at 100- 300 m. Most of the deeper MLD are located to the south of 40 °S, where there is no noticeable thermocline in August and the vertical temperature variation is not evident. It indicates that the thermocline disappears rapidly in this region. Figure 8 (a2) displays the variation of the mean MLD with latitude. The MLD gradually deepens from 60 °N to 40 °N, and

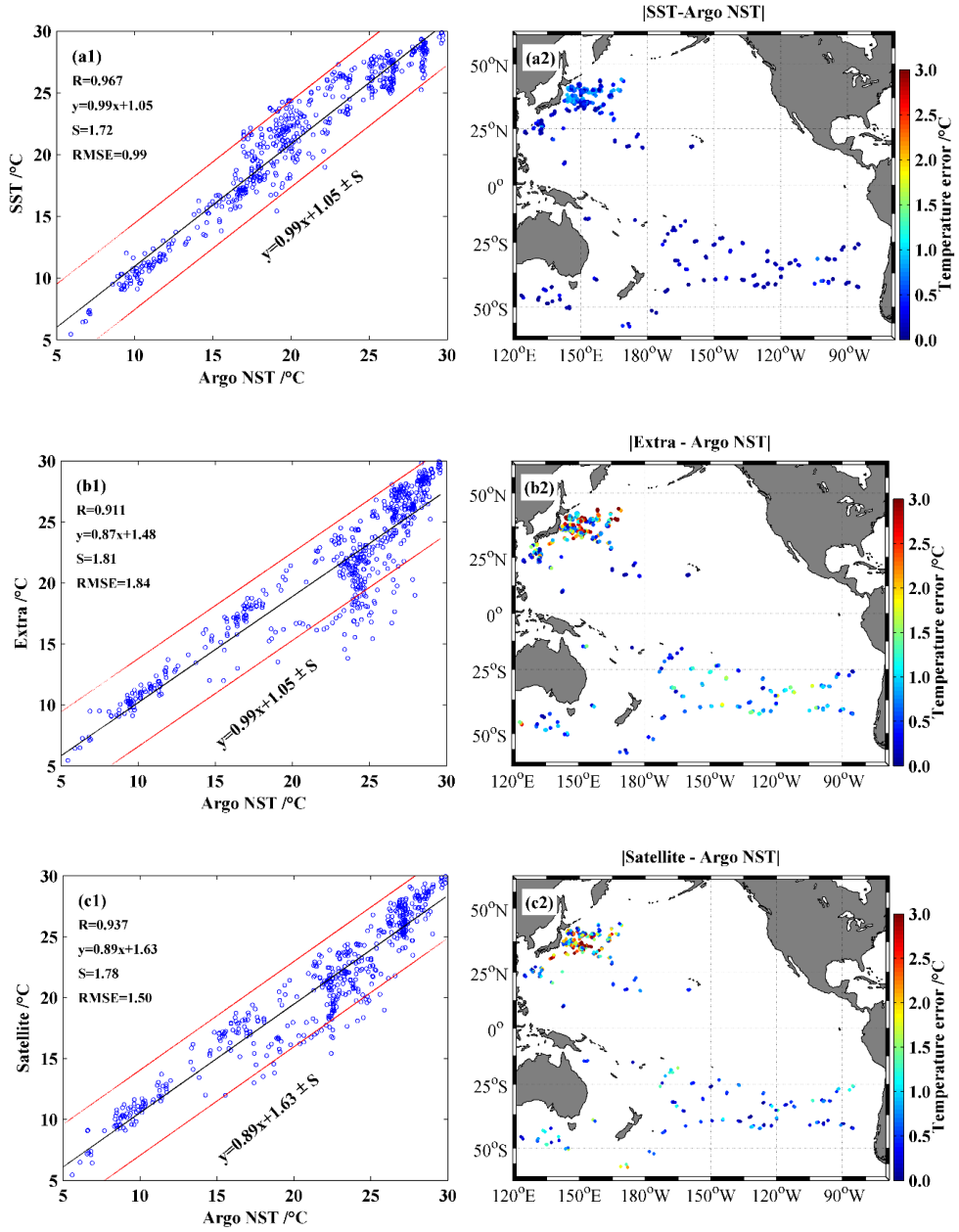

Figure 6. Scatter diagrams of correlation analysis (a1, b1, c1) and absolute temperature errors (a1, a2, a3) between different results and the Argo NST observation. The results of SST obtained using thermocline model, extra obtained by extrapolation, and satellite surface temperature are represented by **(a), (b)**, and **(c)**, respectively. The red lines represent the 95% confidence interval of the regression line (black line) with the residual standard deviation (indicated by S). The correlation coefficient is represented by R.

become shallow in the subarctic. The mean MLD is lower than 50 m in the northern Pacific, and has a value of more than 100 m in the 40 °S–60 °S. These results agree with previous studies [23,26,27]. Thermocline bottom depth is deeper than 100 m, and has higher values in the southern Pacific shown in Figure 8 (c). Its zonal mean value represents increasing trend from north to south similar to the MLD. During August, the thermocline is evident in the northern Pacific. The corresponding TBD is also shallow with a mean value of <200 m. The southern Pacific is characterized by a deeper TBD with a zonal mean value of 300-500 m, and it is even deeper than 800 m at approximately 45 °S. On the other hand, the TBD is ~300 m in the equatorial Pacific.

Temperature gradient represents the strength of the thermocline. Figure 8 (b) illustrates the distribution of TTG and its zonal average. TTG varies from 0 to 0.15 °C/m. TTG is higher than 0.09 °C/m in the tropical Pacific region of 10 °S–10 °N (Figure 8 (b1)). Compared to southern Pacific, the TTG is stronger in most of the northern Pacific region, especially in the regions between 45 °N and 25 °N, where the TTG is generally higher than 0.06 °C/m. The mean TTGs of the northern Pacific are higher than 0.06 °C/m with a value of 0.15 °C/m at approximately 10 °N, as shown in its zonal mean distribution (Figure 8 (b2)). On the other hand, the southern Pacific has a mean TTG of <0.05 °C/m, and the thermocline is notably weakened in the southern hemisphere. TTG is almost close to zero at south of 40 °S, where there is no apparent thermocline.

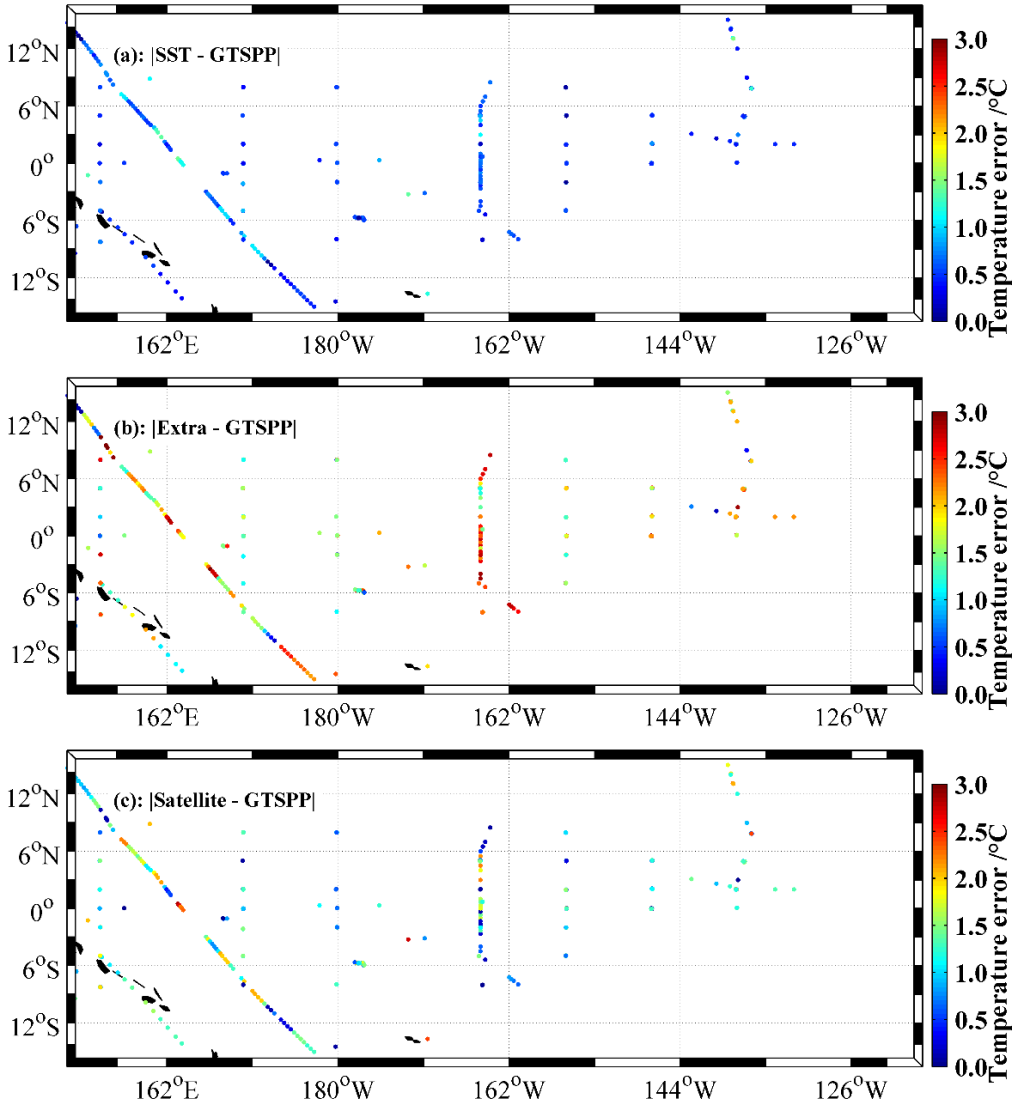

Figure 7. Scatter of absolute temperature errors between thermocline model **(a),** extrapolation **(b)**, and satellite surface temperature **(c)** and GTSPP data.

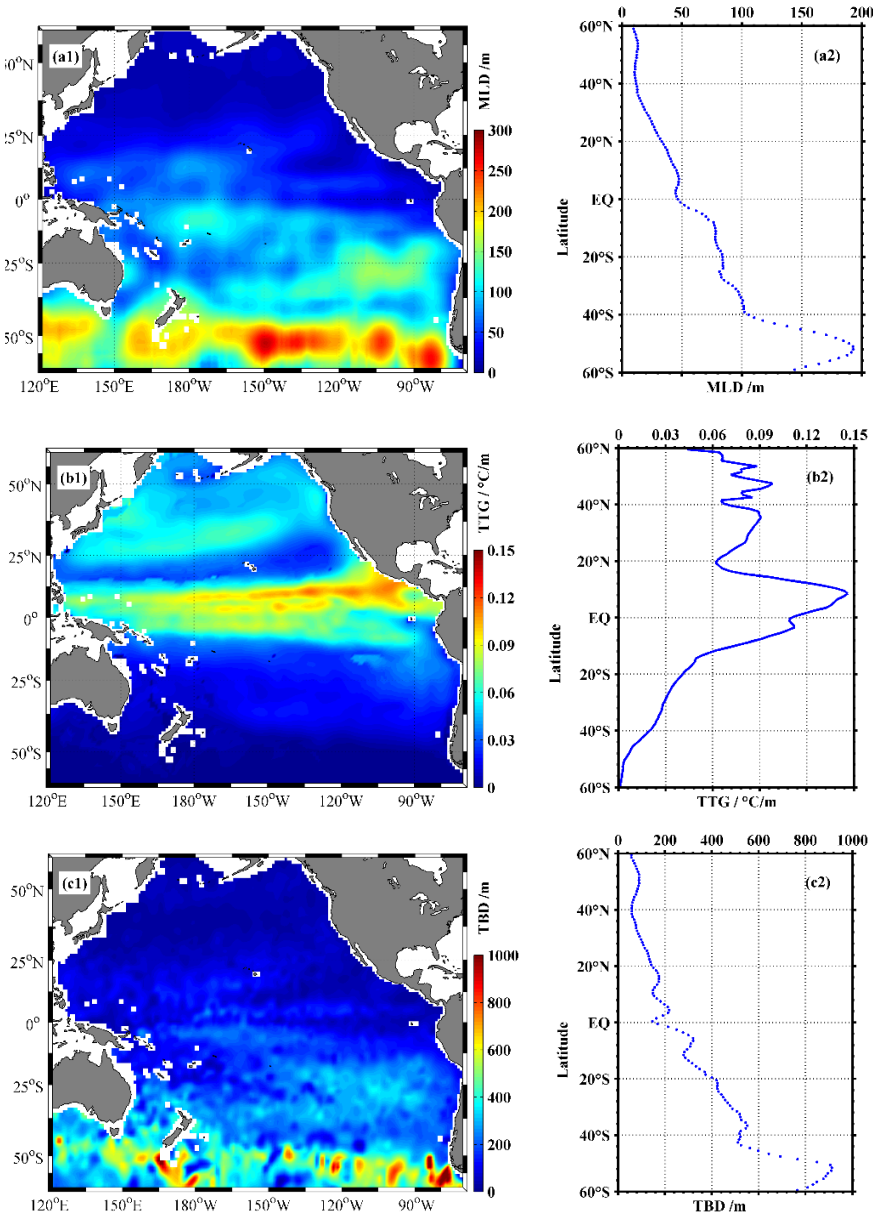

Figure 8. Spatial distribution (a1, b1, c1) and latitude mean (a2, b2, c2) of mixed layer depth **(a)**, thermocline temperature gradient **(b)**, and thermocline bottom depth **(c)**.

4.2 Distribution of Sea Surface Temperature

The thermocline parameter model in section 2.2 provides the monthly distribution of SST. As shown in Figure 9, the surface temperature distribution in the Pacific Ocean shows a trend of increasing temperature in the equatorial region (> 25 °C) and decreasing temperature in the high latitude region. The temperature generally drops below 10 °C in the sub Antarctic and sub polar regions. This reflects the change of solar radiation with latitude. The isotherms are sparse in the range of 20 °S- 20 °N. With temperature transition from the tropics to the polar regions, the isotherms become gradually denser. The isotherms reflect the characters of the polar front at approximately 40 °latitudes. The eastern isotherm between 40 °S and 40 °N bends to low latitudes under the influence of cold current. On the other hand, the western isotherm bends to high latitudes under the influence of warm current. To the south of 40 °S, the isotherm is almost parallel to the latitude. There exists evident warm pool in the equatorial region of the Western Pacific. The center of the warm pool (29 °C isotherm) lies between 5 °S–25 °N during August. These characteristics are consistent with the results obtained from historical observation data and have the potential to extract mesoscale information completely.

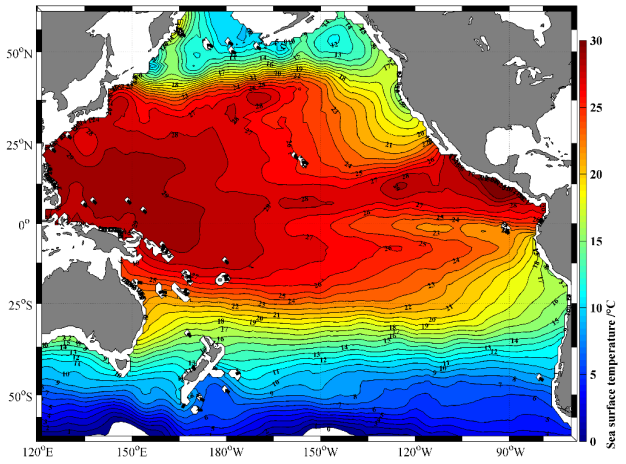

Figure 9. Distribution of the sea surface temperature during August, 2020 in the Pacific Ocean.

5. Conclusions

As one of the important constituents of the global ocean observation system, Argo floats collect temperature and salinity data of upper global ocean rapidly, accurately, and extensively. Argo profiles are increasing at the rate of one hundred thousand sections each year. Meanwhile, SST is an important parameter for both ocean circulation and climate change studies, and several studies rely on complete three-dimension temperature information. Therefore, estimating the Argo SST using available statistic methods has major practical and scientific significance. Based on a thermocline parametric model, the maximum angle method has been used in this study to calculate the model parameters (MLD, TTG and TBD), and subsequently, SST was estimated using Argo subsurface temperature. The estimated results were compared with near surface temperature observations, and were theoretically tested using correlation analysis. The results illustrate that the estimated SSTW is reliable and credible.

In this paper, the maximum angle method was adopted to determine the model parameters (MLD, TTG and TBD). This method is novel, and has stronger theoretical foundation compared to previous methods (e.g. gradient criterion and curvature method). The mixed layer depth obtained by this method is realistic. While using the maximum angle method, the analysis variable should be strictly monotonous. Therefore, the density mixed layer was considered as temperature mixed layer depth in this study. Since the barrier layer was ignored, it is expected to generate certain errors in our model. It is possible to reduce such errors by adopting the temperature profile and combining data from other models in the regions with existing barrier layers.

In addition, the thermocline model employed in this study provides the function between SST and subsurface temperature based on the determined parameters MLD, TTG, TBD etc. For this reason, the accuracy of SST estimated using this method is expected to be relatively lower when the thermoclines are not distinct. Further research is required to overcome these shortcomings. Since the Pacific Ocean was considered as an experimental region to verify the effectiveness of this thermocline model, our study provides a new idea for the construction of Argo SST model in global ocean.

Author Contributions

Conceptualization, C.Z. and C.W.; methodology, C.Z., Z.W., and C.W.; validation, M.Z., D.W., and S.H.; formal analysis, C.Z. and C.W.; investigation, C.Z.; resources, C.Z; writing original draft preparation, C.Z. and C.W.; writing—review and editing, Z.W. and S.H.; visualization, M.Z. and D.W.; funding acquisition, C.Z. All authors have read and agreed to the published version of the manuscript.

Funding

This research was funded by the National Nature Foundation nos. 4210060098, the Argo buoy project under Grant D-8006-21-0082, the Foundation of Key Laboratory of ocean fishery development under Grant A1-2006-21-200201, and the Foundation of fishery resources Comprehensive Scientific Surveys in the Northwest Pacific D-8021-21-0109-01.

Data Availability Statement

Three categories of data used to support the results of this study are included in the article. Argo float data were collected and made freely available by the China Argo Real-time Data Center (ftp://ftp.argo.org.cn/pub/ARGO/global/). Argo NST observation data of the same period are available on the National Oceanography Centre's (NOC) ftp website (ftp://ftp.pol.ac.uk/pub/bodc/argo/NST/). The GTSPP profiles are obtained from National Oceanic and Atmospheric Administration (NOAA) (http://data.nodc.noaa.gov/gtspp/best.nc/).

Acknowledgments

We are grateful to the anonymous reviewers for critically going through the manuscript and for providing necessary comments. We also thank Prof. Chu P of Department of Oceanography, Naval Postgraduate School for several beneficial discussions. Xu Jianping

of the Second Institute of Oceanography is thanked for his comments and English revision. We wish to thank the colleagues at the China Argo Real-time Data Center for numerous presentations and informal discussions that led to the successful implementation of the work presented here. We thank Wiley Editing Services (www.wileyauthors.com/eeo/preparation) for editing this manuscript.

References

[1] Jordi, A., Wang, D.P., 2012. Sbpom: a parallel implementation of prince ton ocean model. Environ. Modell. Softw. 38, 59-61.

[2] Donlon, C., Casey, K., Robinson, I., Gentemann, C., Reynolds, R., Barton, I., Arino, O., Stark, J., Rayner, N., LeBorgne, P., Poulter, D., Vazquez-Cuervo, J., Armstrong, E., Beggs, H., Llewellyn-Jones, D., Minnett, P., Merchant, C., Evans, R., 2009. The GODAE high-resolution sea surface temperature pilot project. Oceanography. 22, 34-45.

[3] Guinehut, S.P., Traon Le, P.Y., Larnicol, G., Philipps, S., 2004. Combining Argo and remote-sensing data to estimate the ocean three-dimensional temperature fields - A first approach based on simulated observations. Journal of Marine Systems. 46, 85-98.

[4] Souza, J.M., Boyer Montegut, A.C., Cabanes, C., Klein, P., 2011. Estimation of the Agulhas ring impacts on meridional heat fluxes and transport using ARGO floats and satellite data. Geophysical Research Letters. 38, L21602.

[5] Hobbs, W.R., Willis, J.K., 2012. Mid latitude North Atlantic heat transport: A time series based on satellite and drifter data. Journal of Geophysical Research. 117, C01008.

[6] Larson, N.L., Janzen, C.D., Murphy, D.J., 2008. STS: An instrument for extending ARGO temperature and salinity measurements through the sea surface. Florida: Poster Presentation Ocean Sciences Meeting. 2008, 2-7.

[7] Xu, J.P., Liu, Z.H., 2007. The experiment of China Argo ocean observing array. Beijing: China Meteorological Press. 4-5.

[8] Chang-Xiang, Y., Jiang, Z., Ji-Ping, X., 2010. An ocean reanalysis system for the joining area of Asia and Indian-Pacific Ocean. Atmospheric and Oceanic Science Letters. 3, 81-86.

[9] Zweng, M.M., Reagan, J.R., Antonov, J.I., Locarnini, R.A., Mishonov, A.V., Boyer, T.P., Garcia, H.E., Baranova, O.K., Johnson, D.R., Seidov, D., Biddle, M.M., 2013. World ocean atlas 2013. Salinity. Ed.; S Levitus. Volume 2.

[10] Martin, M.J., Hines, A., Bell, M.J., 2007. Data assimilation in the FOAM operational short-range ocean forecasting system: A description of the scheme and its impact. Quarterly Journal of the Royal Meteorological Society. 133, 981-995.

[11] Hosoda, S., Ohira, T., Nakamura, T., 2008. A monthly mean dataset of global oceanic temperature and salinity derived from Argo float observations. JAMSTEC Report. Research Developments. 8, 47-59.

[12] Gaillard, F., 2010. ISAS-Tool version 5.3: Method and configuration. Laboratoere de Physique de Oceans. UMR6523, 1-12.

[13] Brion, E., Gaillard, F., 2012. ISAS-Tool version 6: User's manual. Report LPO 01-12. 2012, 1-45.

[14] Roemmich, D., Gilson, J., 2009. The 2004-2008 mean and annual cycle of temperature, salinity, and steric height in the global ocean from the Argo Program. Progress in Oceanography. 82, 81-100.

[15] Wang, H.Z., Wang, G.H., Zhang, R., A., Y.Z., Jin, B.G., 2010. User's Manual of User's Manual of Argo Gridded Salinity Product (G-Argo). Hangzhou: Second Institute of Oceanography. 1-6.

[16] Li, H., Xu, F., Zhou, W., et al., 2017. Development of a global gridded Argo data set with Barnes successive corrections. Journal of Geophysical Research: Oceans. 122, 866-889.

[17] Shi, M.Ch., Gao, G.P., Bao, X.W., 2000. Method of ocean survey. Qingdao: Qingdao Ocean University Press. 51-52.

[18] Lu, S.L., Xu, J.P., Liu, Z.H., 2014. Analysis of the differences between microwave remote sensing SST and Argo NST in the Southern Hemisphere. Marine Forecasts. 31, 1-8.

[19] Liu, Z., Xu, J., Zhu, B., et al., 2006. Calibration of Argo profiling float salinity data using historical hydrographic data[A]. Hangzhou. Proceedings of "China Argo Science Workshop" Conference. 14-17.

[20] Chu, P.C., Fan, C.W., Liu, W.T., 2000. Determination of vertical thermal structure from sea surface temperature. Journal of Atmospheric and Oceanic Technology Meteorological Society. 17, 971-979.

[21] Chu, P.C., Fan, C.W., 2011. Maximum angle method for determining mixed layer depth from sea glider data. Journal of Oceanography. 67, 219-230.

[22] Zhang, C.L., Xu, J.P., Bao, X., 2015. Gradient dependent correlation scale method based on Argo. Journal of PLA University of Science and Technology (Natural Science Edition). 16, 476-483.

[23] Akima, H., 1970. A new method for interpolation and smooth curve fitting based on local procedures. Journal of the ACM. 17, 589-602.

[24] Juza, M., Penduff, T., Brankart, J.M., Barnier, B., 2012. Estimating the distortion of mixed layer property distributions induced by the Argo sampling. Journal of Operational Oceanography. 5, 45-58.

[25] Zhang, C.L., Xu, J.P., Bao, X., et al., 2013. An effective method for improving the accuracy of Argo objective analysis. Acta Oceanologica Sinica. 32, 66-77.

[26] Zhang, C.L., Wang, Z.F., Liu, Y., 2021. An argo-based experiment providing near-real-time subsurface oceanic environmental information for fishery data. Fisheries Oceanography. 30, 85-98.

[27] Lu, J., Qiao, F.L., Wei, Z.X., Teng, Y., Xia, C.Sh., 2008. Study on distribution of mixed layer depth in the world ocean in summer. Advances in Marine Science. 26, 145-155.